Fingerprinting Petroporphyrin Structures with Vibrational Spectroscopy. 3. Resonance Raman Characterization of Regioisomers of Nickel(II) Tetrahydrobenzoetioporphyrin

J. Graham Rankin,[†,‡] Roman S. Czernuszewicz,[*,†] and Timothy D. Lash[§]

Departments of Chemistry, University of Houston, Houston, Texas 77204, and Illinois State University, Normal, Illinois 61761

Received January 10, 1994[⊗]

Nickel(II) complexes of the geochemically significant four regioisomers of tetrahydrobenzoetioporphyrin, NiTHBP-A, -B, -C, and -D, which contain a reduced benzo unit fused onto the C_β atoms of a pyrrole ring, have been synthesized and structurally characterized by resonance Raman (RR) spectroscopy with variable-wavelength excitation. Spectra were obtained from CS_2 and CH_2Cl_2 solution samples at room temperature excited at 406.7, 530.9, and 568.2 nm, in resonance with the porphyrin Soret, Q_1, and Q_0 electronic transitions, respectively. For comparison, similar RR spectra were measured for Ni(II) tetra-β,β-butanoporphyrin (NiTBuP) in which each pyrrole bears a tetrahydrobenzo exocyclic ring. These three excitation wavelengths, which selectively enhanced vibrational modes of different symmetry, the measured Raman band depolarization ratios, and the already available normal coordinates of Ni(II) octaethylporphyrin (NiOEP) permitted assignment of RR bands to nearly all of the porphyrin in-plane skeletal modes. The frequencies of skeletal modes above 1300 cm^{-1} indicate more planar structures in solution for NiTHBP's and NiTBuP relative to NiOEP and Ni(II) etioporphyrins. Several unique marker bands are also found for modes of the tetrahydrobenzo exocyclic rings, especially in the 568.2-nm excited spectra. The relative positions of the methyl and ethyl substituents have a marked influenced on the low- (350−550 cm^{-1}) and mid-frequency (750−1100 cm^{-1}) vibrational spectra, allowing the four NiTHBP regioisomers to be readily distinguished.

Introduction

Petroporphyrins (or geoporphyrins) containing mainly nickel(II) and oxovanadium(IV) (vanadyl) bound to a variety of alkylporphyrins are widely distributed in organic-rich sediments such as oil shale and petroleum.[1] These inherent nonvolatile constituents of fossil fuels are believed to be diagenetic remnants of biological pigments, primarily chlorophylls and bacteriochlorophylls.[2,3] Their peripheral substituents have been drastically modified over geological time scales, and the analysis of metalloporphyrins from a given organic-rich sediment can give information about its geochemical history (depositional environment, thermal maturity, etc.).[3] Several major families of petroporphyrins have been identified in petroleum: a polyalkylporphyrin series with simple alkyl groups on the pyrrole-C_β carbon atoms structurally related to etioporphyrin-III (Etio); a series with five-membered exocyclic rings structurally related to deoxophylloerythroetioporphyrin (DPEP) and its *meso*-β-cycloalkanoporphyrin (CAP) homologs with expanded exocycles of six or seven carbon atoms; a rhodo-type series which have been shown to possess a basic β,β-benzoporphyrin skeleton with peripheral substituent motifs of either Etio's (benzoEtio or Benzo) or DPEP's (benzoDPEP).[1]

Monobenzoporphyrins (benzoEtio) and benzoDPEP's (Figure 1) have been identified in relatively immature marine sediments and mature oils of marine origin by mass spectrometry, although the substituent groups and their positions around the macrocycle have not been conclusively determined for benzoEtio's.[3,4] The alkyl substituents of two benzoDPEP's isolated from Boscan oil shale (Venezuela) have been determined by nOe difference

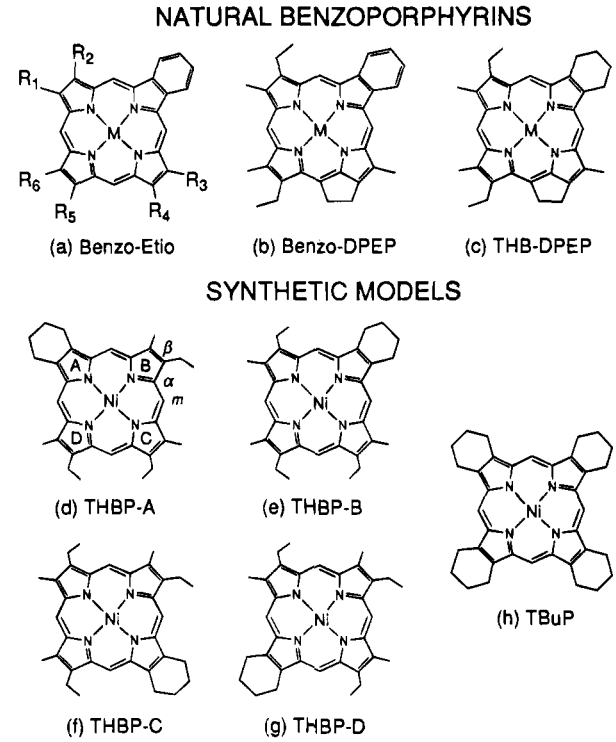

Figure 1. Representative benzo- and tetrahydrobenzoporphyrins from geological sources (a−c) and their synthetic models studied in this work (d−h). Natural petroporphyrins: M = V^{IV}=O (primarily) or Ni(II), (a) benzoporphyrin (R_1−R_6 = unspecified alkyl groups),[3] (b) benzoDEP,[9] and (c) tetrahydrobenzoDPEP.[9] Nomenclature for synthetic porphyrins (d−h) given in the Experimental Section.

* Author to whom correspondence should be addressed.
† University of Houston.
‡ Present address: Department of Chemistry, Marshall University, Huntington, WV 25755.
§ Illinois State University.
⊗ Abstract published in *Advance ACS Abstracts,* May 1, 1995.
(1) Baker, E. W.; Palmer, S. E. In *The Porphyrins*; Dolphin, D., Ed.; Academic Press: New York, 1978; Vol. 1, pp 486−552.
(2) Treibs, A. *Leibigs Ann. Chem.* **1934**, *509*, 103−114.
(3) Baker, E. W.; Louda, J. W. In *Biological Markers in the Sedimentary Record*; John, R., Ed.; Elsevier: Amsterdam, 1986; pp 125−225.

0020-1669/95/1334-3025$09.00/0

proton NMR spectroscopy (Figure 1b).[5] The origin of benzoporphyrins in petroleum is not presently known; however, tetrahydrobenzoporphyrins (THBP) containing a reduced benzo unit fused onto the C_β atoms of a pyrrole ring have been proposed as the diagenetic precursors to these compounds.[1,3] Tetrahydrobenzo derivatives of DPEP (THB-DPEP, Figure 1c) have been isolated from immature sediments as vanadyl complexes and as free-bases.[4a,6,7] An alternative scheme has been devised by Quirke *et al.*,[4a] who postulated that both the benzo- and tetrahydrobenzoporphyrins are derived from a common cyclohexyldiene precursor which could be either completely aromatized to the Benzo or be reduced to the THBP. Recently, a likely case was made for divinylchlorophyll *a*, a widespread pigment in marine algae, as being the biological precursor to many of the benzo- and tetrahydrobenzoporphyrins from oil shales and petroleum.[8,9]

Although the tetrahydrobenzo analogs of benzoEtio's (THBP's) have not been isolated from either sediments or petroleum, the four possible isomers of a free-base THBP (Figure 1d−g) have recently been synthesized.[8] These four isomers have one methyl and one ethyl at the β-pyrrole positions on each of three pyrrole rings with the β,β-butano substituent on the fourth. The four isomers can be "derived" from Etio-III by replacing the alkyl substituents with the exocycle on each of the four pyrrole rings (A−D). A fifth free-base THBP structure, tetra-β,β-butanoporphyrin (TBuP), has also been synthetically accessed,[8] in which the β-pyrrole carbons of each pyrrole are connected by butano chain to give six-membered rings (Figure 1h).

No X-ray structures are available for any of these compounds, but it is logical to assume that the bridging butano group will adopt a nonplanar half-chair configuration similar to that of cyclohexene.[10] Recently, Shelnutt *et al.*[11] synthesized the tetra-β,β-butano derivative of nickel tetraphenylporphyrin (they abbreviated as $NiTC_6TPP$) and reported that the preliminary X-ray structure of the porphyrin macrocycle was highly nonplanar, most likely due to the steric interaction between the phenyl groups and the exocycle rings. An energy-optimized structure of $NiTC_6TPP$ has been derived by these workers from molecular mechanics calculations that suggests a half-chair configuration of the tetrahydrobenzo rings in $NiTC_6TPP$. The X-ray structure of nickel tetra-β,β-propanotetraphenylporphyrin ($NiTC_5TPP$), the five-membered exocyclic ring analog of $NiTC_6$-TPP, showed the β,β-cycloalkano rings to be coplanar with the porphyrin macrocycle.[12]

The application of resonance Raman (RR) spectroscopy has become an important source of information about the structure and dynamics of tetrapyrrole-containing protein complexes and their model compounds, metalloporphyrins.[13,14] Recognizing its potential as an aid to the ongoing structure determination studies of metalloporphyrins in organic-rich sediments, we have recently initiated extending the technique to major structural types of petroporphyrins found in oil shales and petroleum. In the first paper of this series,[15a] we demonstrated that the RR scattering can be a powerful tool in elucidating slight structural perturbations for nickel and vanadyl etioporphyrins I and III due to central metal ions and relative positions of the methyl and ethyl substituents on the different pyrrole rings. Subsequently we have extended this study to all four NiEtio positional isomers and found distinctively unique vibrational signatures for each isomer in the 700−1100-cm^{-1} spectral region.[15b] In the present work, the Ni(II) complexes of the four regioisomers of tetrahydrobenzoetioporphyrin (NiTHBP-A−D) are characterized for the first time by using a variable-wavelength excitation RR spectroscopy as a probe of structure. The spectra of NiTBuP having a β,β-butano group on each pyrrole were also recorded to obtain peak positions for the tetrahydrobenzo exocyclic ring. Vibrational band assignments are made based on comparison with the well-understood NiOEP (OEP = octaethylporphyrin).[16] In addition, RR spectra of NiTBuP, both the natural abundance (na) and the *meso*-d_4 isotopomer (NiTBuP-d_4), and the *meso*-d_4 isotopomer of NiTHBP-C (NiTHBP-C-d_4) were used to support band assignments. Particular effort is made to establish structure marker band(s) for the tetrahydrobenzo exocycle and to determine distinguishing features of the RR spectra of the four NiTHBP regioisomers. In the next paper,[17] we will report the RR marker bands unique to nickel(II) cycloalkanoporphyrins, which bear a saturated carbon ring on the porphyrin macrocycle C_m and C_β carbons, and describe the structural effects of exocycle ring size (five to seven carbons) on the porphyrin skeletal vibrations in the CAP family.

Experimental Section

Materials and Methods. The free-bases of the tetrahydrobenzoporphyrin isomers A−D (THBP-A = 2,3-butano-8,13,17-triethyl-7,12,-18-trimethylporphyrin; THBP-B = 7,8-butano-3,13,17-triethyl-2,12,18-trimethylporphyrin; THBP-C = 12,13-butano-3,8,17-triethyl-2,7,18-trimethylporphyrin; THBP-D = 17,18-butano-3,8,13-triethyl-2,7,12-trimethylporphyrin) and a tetra-β,β-butanoporphyrin (TBuP = 2,3:7,8:12,13:17,18-tetrabutanoporphyrin) were synthesized and purified as described previously.[8,18] Nickel was incorporated by refluxing the respective free-base porphyrin with nickel acetate in hot (150 °C) dimethylformamide (DMF).[19] The dried solids were chromatographed on thin layer silica gel plates (250 μm thick Absorbosil, Alltech, Deerfield, IL) with hexane/methylene chloride of 3:1 (v/v) ratio or pure carbon disulfide (Aldrich, Milwaukee, WI). Yields following chromatography were approximately 80%. All solvents were reagent grade or better (HPLC grade, Spectranalyzed, etc.).

Deuterium exchange of the methine bridge hydrogens (d_4) in NiTBuP and NiTHBP-C was carried out by reacting the respective free-base

(4) (a) Quirke, J. M. E.; Dale, T.; Britton, E. D.; Yost, R. A.; Trichet, J.; Belayouni, H. *Org. Geochem.* **1990**, *15*, 169−177. (b) Quirke, J. M. E. In *Metal Complexes in Fossil Fuels*; Filby, R. H., Branthaver, J. F., Eds.; ACS Symposium Series 344; American Chemical Society: Washington, DC, 1987; pp 308−331.
(5) Kaur, S.; Chicarelli, M. I.; Maxwell, J. R. *J. Am. Chem. Soc.* **1986**, *108*, 1347−1348.
(6) Filby, R. H.; Van Berkel, G. J. In *Metal Complexes in Fossil Fuels*; Filby, R. H., Branthaver, J. F., Eds.; ACS Symposium Series 344; American Chemical Society: Washington, DC, 1987; pp 2−39.
(7) (a) Verne-Mismer, J.; Ocampo, R.; Bauder, C.; Callot, H. J.; Albrecht, P. *Energy Fuels* **1990**, *4*, 639−643. (b) Verne-Mismer, J.; Ocampo, R.; Callot, H. J.; Albrecht, P. *J. Chem. Soc., Chem. Commun.* **1987**, 1581−1583.
(8) May, D. A.; Lash, T. D. *J. Org. Chem.* **1992**, *57*, 4820−4828.
(9) Lash, T. D. *Energy Fuels* **1993**, *7*, 166−171.
(10) Beckett, C. W.; Freeman, N. K.; Pitzer, K. S. *J. Am. Chem. Soc.* **1948**, *70*, 4227−4230.
(11) Shelnutt, J. A.; Medforth, C. J.; Berber, M. D.; Barkigia, K. M.; Smith, K. M. *J. Am. Chem. Soc.* **1991**, *113*, 4077−4087.
(12) Medforth, C. J.; Senge, M. O.; Smith, K. M.; Sparks, L. D.; Shelnutt, J. A. *J. Am. Chem. Soc.* **1992**, *114*, 9859−9869.
(13) *Biological Applications of Raman Spectroscopy*; Spiro, T. G., Ed.; Wiley: New York, 1988; Vol. 3.
(14) Spiro, T. G.; Czernuszewicz, R. S.; Li, X.-Y. *Coord. Chem. Rev.* **1990**, *100*, 541−571.
(15) (a) Rankin, J. G.; Czernuszewicz, R. S. *Org. Geochem.* **1993**, *20*, 521−538. (b) Rankin, J. G.; Czernuszewicz, R. S.; Lash, T. D. *Org. Geochem.*, in press.
(16) (a) Li, X.-Y.; Czernuszewicz, R. S.; Kincaid, J. R.; Stein, P.; Spiro, T. G. *J. Phys. Chem.* **1990**, *94*, 47−61. (b) Czernuszewicz, R. S.; Li, X.-Y.; Spiro, T. G. *J. Am. Chem. Soc.* **1989**, *111*, 7024−7031. (c) Li, X.-Y.; Czernuszewicz, R. S.; Kincaid, J. R.; Spiro, T. G. *J. Am. Chem. Soc.* **1989**, *111*, 7012−7023.
(17) Rankin, J. G.; Czernuszewicz, R. S.; Lash, T. D. To be submitted for publication.
(18) Lash, T. D. *Org. Geochem.* **1989**, *14*, 213−225.
(19) Adler, A. D.; Longo, F. R.; Kampas, F.; Kim, J. *J. Inorg. Nucl. Chem.* **1970**, *32*, 2443−2445.

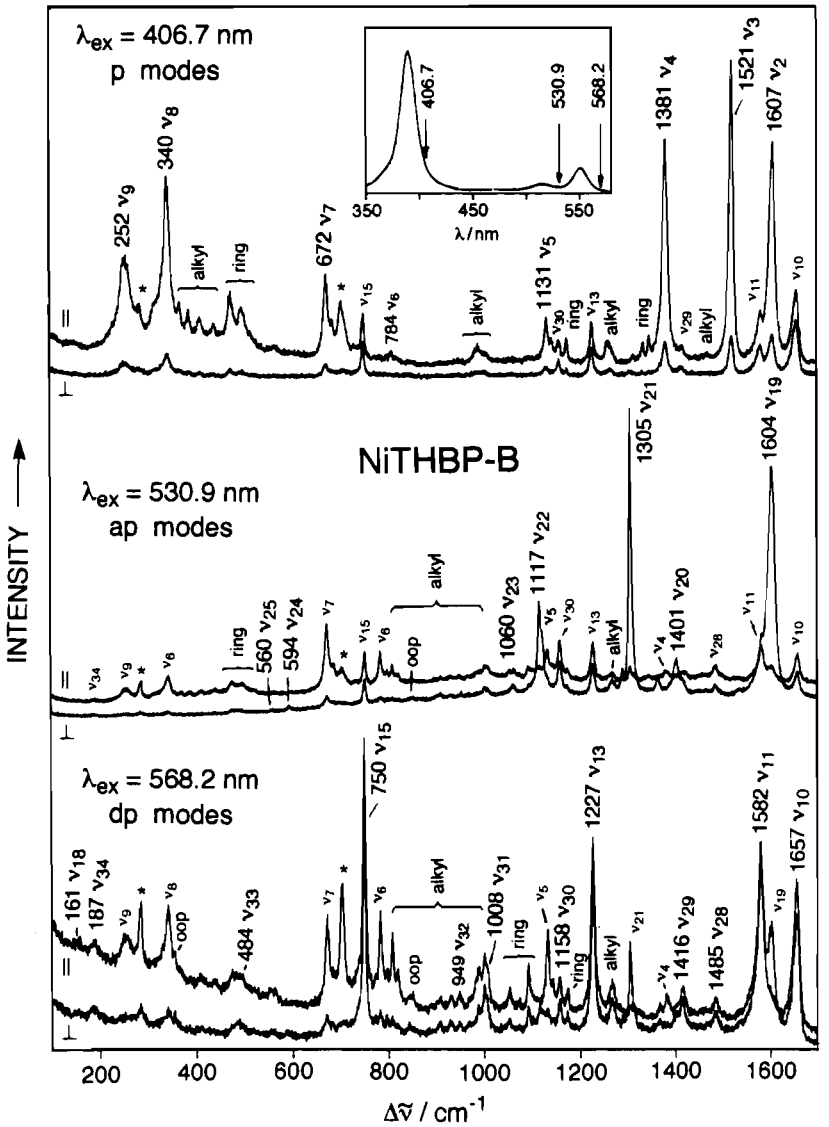

Figure 2. RR spectra in parallel (||) and perpendicular (⊥) scattering of NiTHBP-B (~1 mM) in CH_2Cl_2 at the three indicated excitation wavelengths, which bring out selectively the A_{1g} (p) (406.7 nm), A_{2g} (ap) (530.9 nm), and B_{1g}, B_{2g} (dp) (568.2 nm) porphyrin skeletal vibrational modes, whose assignments are given by the labels (alkyl and ring = substituent modes; see text). Solvent bands are indicated with asterisks. Conditions: backscattering from spinning NMR tube; 150-mW laser power; 3-cm^{-1} slit widths; one scan, 1-s integration time per data point at 1-cm^{-1} increments. Inset: UV−visible spectrum of NiTHBP-B in CH_2Cl_2 (arrows indicate excitation wavelengths used for RR measurements).

porphyrin with ~90% wt D_2SO_4 for 48 h at room temperature[20] followed by the metal insertion reaction.[19] Due to limited sample quantity only these two compounds were isotopically labeled. Concentrated (98% wt) deuterated sulfuric acid (99.5% D, Aldrich) was diluted 9:1 by volume with deuterated water (99.96% D, Aldrich). After 48 h, the reaction mixture was poured over ~50 g of ice and the porphyrin extracted into methylene chloride (50 mL). The organic layer was washed with saturated $NaHCO_3$ solution (50 mL) and deionized water (3 × 50 mL) and then evaporated with a stream of nitrogen. The exchange reaction was complete in one pass as judged by the disappearance of the *meso*-H signal (~10 ppm) in the proton NMR spectrum. Nickel insertion into the free-base porphyrin-*meso*-d_4 was performed by the DMF method described above.

Spectroscopic Measurements. The RR spectra of petroporphyrins were obtained with a Coherent K-2 cw krypton ion laser excited at or near the absorption maxima of the porphyrin Soret and Q bands with 406.7 (violet), 530.9 (green), and 568.2 nm (yellow) lines. Typical laser power was 100−200 mW. Essentially all of the Raman-active fundamental modes can be identified in the spectra by using these three excitation wavelengths. The scattered photons were collected via 135° backscattering geometry for spinning NMR tubes[21] in solution (~1 mM in methylene chloride or carbon disulfide). For all spectral runs, a quartz wedge (polarization scrambler) was placed before the monochromator entrance slit. Its function is to change linear into circular polarization of the light entering the slit to avoid measurement errors due to the variable spectrometer transmittance of the light polarized in different directions. To obtain the depolarization ratios, $\rho = I_\perp/I_\parallel$, of the Raman bands, a polarizing filter (analyzer) was used for all spectra aligned either parallel or perpendicular to the electric vector of the scattered light. A Spex 1403 double monochromator, equipped with 1800 grooves/mm holographic gratings and a Hamamatsu 928 photomultiplier detection system, was used to record all the spectra under the control of a Spex DM3000 microcomputer system.[22] External (entrance and exit) slit settings were determing from a published table[23] for the Spex 1403 instrument or by experimentation to give a spectral bandpass of 2 cm^{-1} (530.9 or 568.2 nm) or 3 cm^{-1} (406.7 nm). Internal

(20) Fuhrhop, J. H.; Smith, K. M. In *Porphyrins and Metalloporphyrins*; Smith, K. M., Ed.; Elsevier: New York, 1975; pp 757−869.

(21) (a) Walters, M. A. *Appl. Spectrosc.* **1993**, *37*, 299−300. (b) Eng, J. F.; Czernuszewicz, R. S.; Spiro, T. G. *J. Raman Spectrosco.* **1985**, *16*, 432−437.

(22) Czernuszewicz, R. S. In *Methods in Molecular Biology*; Jones, C., Mulloy, B., Thomas, A. H., Eds.; Humana Press: Totowa, NJ, 1993; Vol. 17, Chapter 15, pp 345−374.

(23) Strommen, D. P.; Nakamoto, K. *Laboratory Raman Spectroscopy*; Wiley: New York, 1984.

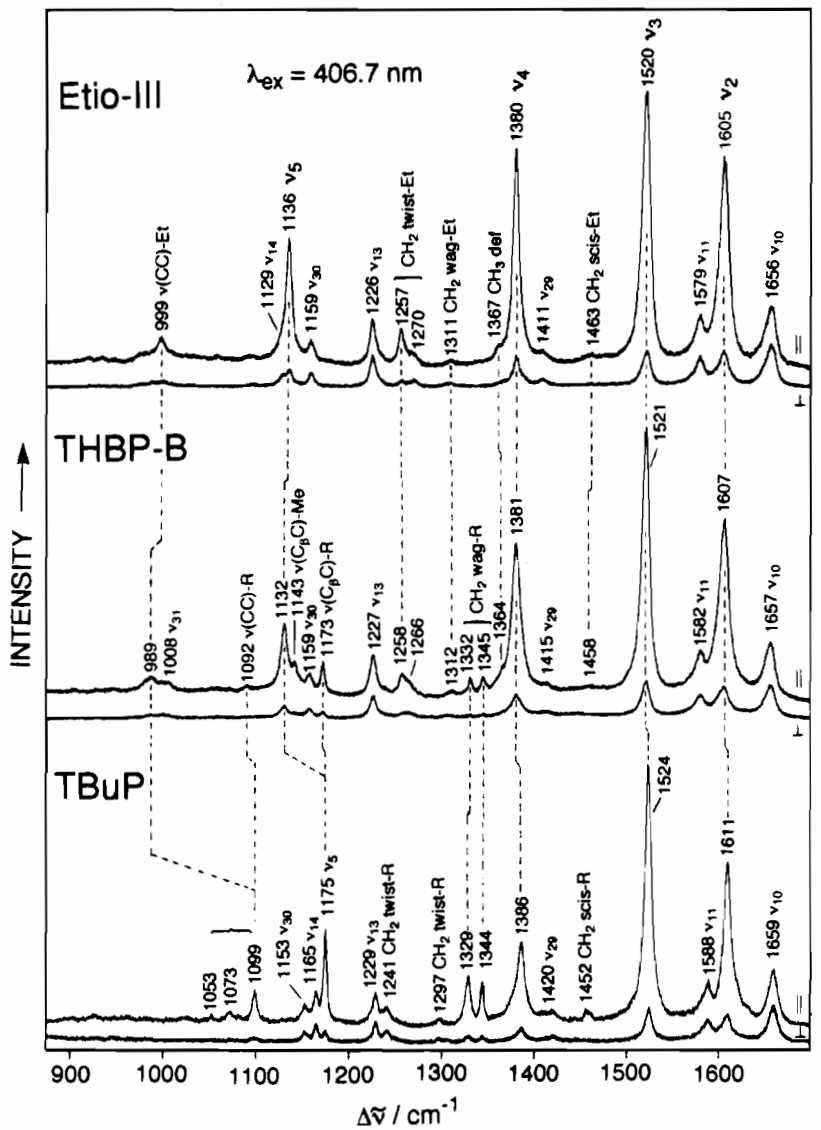

Figure 3. 406.7-nm-excited RR spectra in CS_2 of NiEtio-III (top), NiTHBP-B (middle), and NiTBuP (bottom) in the 850−1700 cm^{-1} region, where the most prominent porphyrin skeletal modes occur. Polarized (A_{1g}) bands are correlated. Conditions: backscattering from spinning NMR tube; 150-mW laser power, 3-cm^{-1} slit widths; average of three scans, 1-s integration time per data point at 0.5-cm^{-1} increments.

slit settings were 500 μm for all laser lines. Raman data were obtained at 1-cm^{-1} increments over the range of 100-1700 cm^{-1} for the survey spectra and at 0.5-cm^{-1} increments over smaller ranges for detailed spectra. Integration times for single scans were 1 s per data point for all spectra. Multiple scans (2−4) were averaged to improve signal to noise ratio. Raman data manipulation was performed using LabCalc software (version A2.23; Galactic Industries, Inc.) on a 486-DX 33 MHz PC microcomputer. Solvent bands were routinely subtracted using reference spectra collected under identical conditions of scan rate and slit width utilizing the LabCalc subroutines. The quality of the observed Raman signal was sufficiently high that no baseline correction or smoothing was required, and all the plots shown in this work are on the uncorrected data. A Hewlett-Packard 8-pen ColorPro graphics plotted was used for hard copy output of spectra.

Optical absorption spectra were obtained in methylene chloride with 1-mm quartz cell using an HP-8542 diode array spectrophotometer. The concentration of each metalloporphyrin was adjusted such that the maximum absorbance of the Soret band was about 1 absorbance unit. Resolution of the spectra was 2 nm. λ_{max} (in CH_2Cl_2) (nm): NiTHBP-A, 389.5, 514.8, 550.9; NiTHBP-B, 389.5, 514.9, 550.9; NiTHBP-C, 389.5, 514.8, 550.9; NiTHBP-D, 389.5, 514.9, 550.9; NiTBuP, 389.0, 514.6, 550.6.

Proton NMR spectra were obtained on a General Electric QE-300 Fourier transform NMR at 300 MHz in deuterated chloroform with 0.3% tetramethylsilane (TMS) as a reference (Aldrich). Eight to thirty-two scans gave sufficient signal-to-noise for analysis. The concentration of the porphyrin was ~1 mM in $CDCl_3$.

Results and Discussion

Electronic Spectra and RR Enhancement Pattern. Essentially no difference in the electronic spectra was seen over the range of 300−700 nm among the four regional isomers of NiTHBP either in the positions of the absorption bands or their corresponding absorbances. There is a very small (<1 nm) shift to higher energy of the Soret and Q-bands going to NiTBuP, however (see Experimental Section). Each spectrum, as exemplified by that of isomer B in the inset of Figure 2, showed the classical very intense Soret band, at ~389 nm, and two weaker Q bands, at ~515 nm (Q_1) and ~551 (Q_0), which arise from a strong configuration interaction and vibronic mixing between the two lowest energy $\pi-\pi^*$ orbital excitations, $a_{2u}(\pi) \rightarrow e_g(\pi^*)$ and $a_{1u}(\pi) \rightarrow e_g(\pi^*)$ (both allowed and of E_u symmetry under the effective D_{4h} point group of the porphyrin chromophore).[24] The UV−vis spectra also closely match those of NiOEP and NiEtio, implying that the exocyclic ring(s) at the pyrrole C_β,C_β positions do not alter the π,π^* orbital energies.

(24) Gouterman, M. In *The Porphyrins*; Dolphin, D., Ed.; Academic Press: New York, 1978; Vol. III, Part A, pp 1−165.

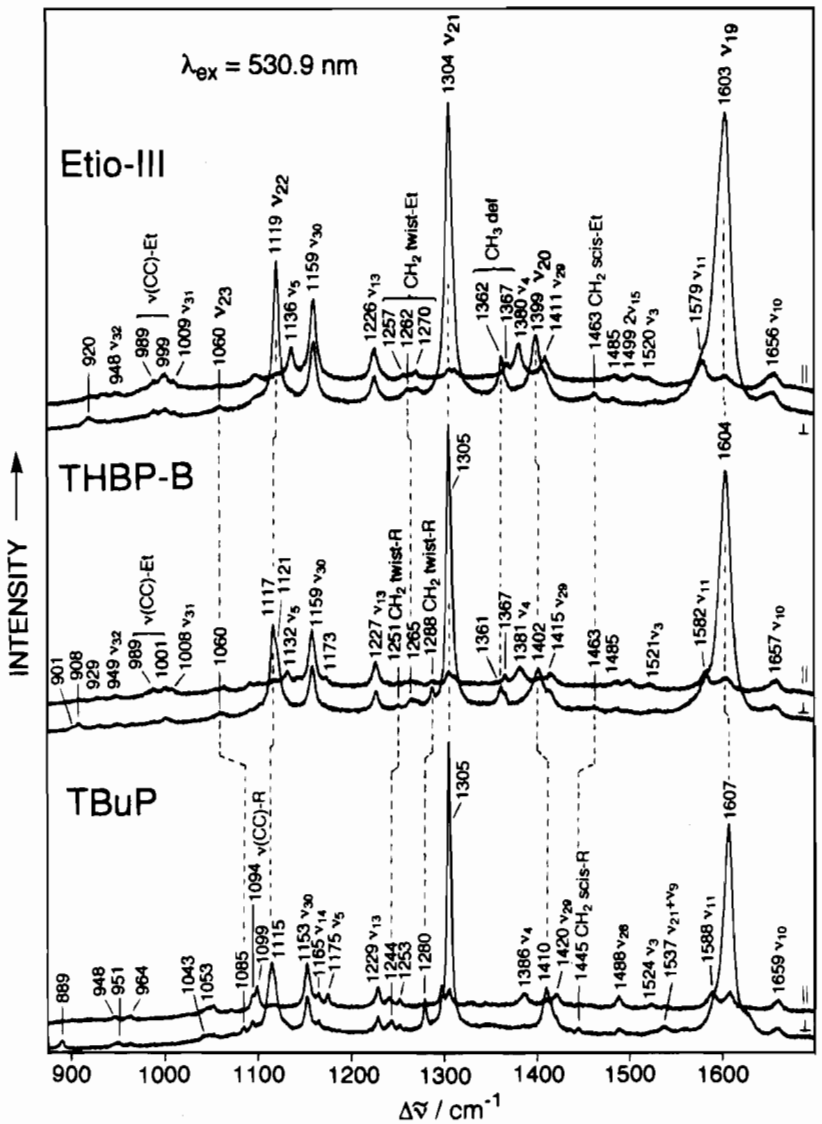

Figure 4. Same as in Figure 3, but with 530.9-nm excitation and 2-cm^{-1} slit widths. Anomalously polarized (A_{2g}) bands are correlated.

Raman excitation into these well-separated Soret and Q excited states results in strong enhancements of the vibrational modes of the porphyrin ring and of peripheral substituents, the relative intensities of which change dramatically with the laser excitation wavelength. This is demonstrated in Figure 2, which shows survey spectra of NiTHBP-B obtained in methylene chloride solution with three difference excitation wavelengths, 406.7 (top), 530.9 (middle), and 568.2 nm (bottom). The survey spectra of the other NiTHBP isomers are not shown because their enhancement patterns are identical to that of NiTHBP-B which is shown in Figure 2. Among the enhanced vibrational modes, the in-plane skeletal porphyrin modes (labeled ν_i) show the largest increase in the intensity, as expected for resonance with the $\pi-\pi^*$ electronic transitions which are also polarized in the porphyrin plane.[14,15] However, the vibrational modes of the ethyl and methyl substituents (labeled "alkyl") as well as several THB ring modes (labeled "ring") also display significant enhancements, especially with the 568.2-nm excitation wavelength. Not only do these modes show substantial intensity but their frequencies are responsive to minute structural perturbations due to the altered positions of the alkyl groups around the porphyrin core (*vide infra*).

Most of the NiTHBP bands in the 406.7-nm-excited spectrum are polarized (p) and arise from totally symmetric vibrational modes which derive their intensity via Franck−Condon (or *A*-term) scattering[25] from the Soret absorption band. [See Discussion in ref 15a, for RR scattering mechanisms of metalloporphyrins.] The high-frequency ν_2, ν_3, and ν_4 skeletal A_{1g} modes, which involve mainly in-plane stretchings of the pyrrole $C_\beta-C_\beta$ (ν_2), methine bridge $C_\alpha-C_m$ (ν_3), and pyrrole $C_\beta-C_\beta/C_\alpha-N$ (ν_4) bonds, give rise to the strongest bands, in analogy to the NiOEP[16a] and NiEtio[15] RR spectra. This dominance is consistent with the expected weakening of the π-bonding in the excited state upon the $\pi-\pi^*$ electronic transition. Also intense in the 406.7-nm spectrum are the skeletal modes ν_8 (~340 cm^{-1}) and ν_9 (~250 cm^{-1}) in the low-frequency region, which are assigned to the strongly coupled Ni−pyrrole breathing and C_β−alkyl bending motions. Similar resonance behavior has previously been observed for NiOEP and NiEtio complexes, although the ν_8 and ν_9 modes of NiOEP differ in that they occur as much weaker characteristic doublets due to ethyl orientational isomerism.[14,16a] The depolarization ratios, $\varrho = I_\perp/I_\parallel$, of the A_{1g} modes are close to the expected value, 1/8, for in-plane electronic transitions in D_{4h} symmetry, indicating that the basic porphyrin core of NiTHBP's retains a highly symmetric porphine-like character.

The Q-state excitation of NiTHBP's (530.9 and 568.2 nm) results in selective resonance enhancement of mainly depolarized

(25) Tang, J.; Albrecht, A. C. *J. Chem. Phys.* **1968**, *49*, 1144−1154.

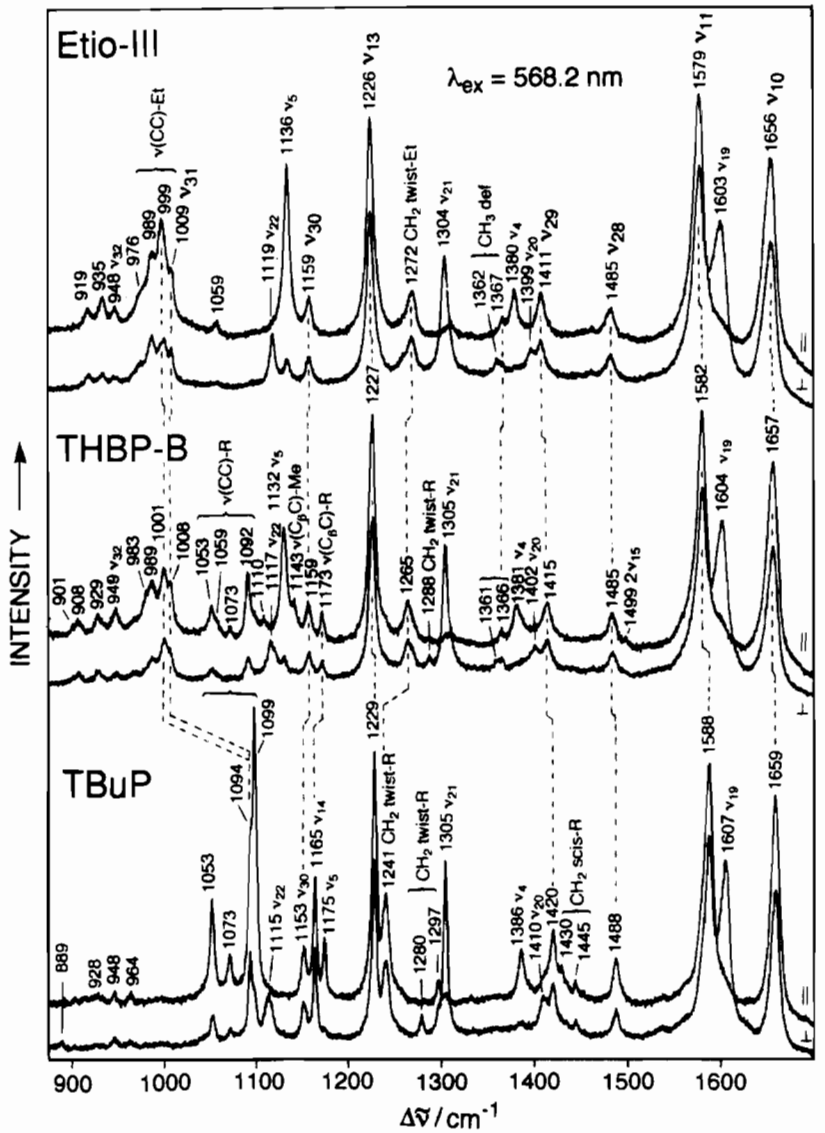

Figure 5. Same as in Figure 3, but with 568.2-nm excitation and 2-cm^{-1} slit widths. Depolarized (B_{1g}, B_{2g}) bands are correlated.

(dp, $\varrho \approx 3/4$) (568.2 nm) or anomalously polarized (ap, $\varrho > 3/4$) (530.9 nm) non-totally symmetric modes, which derive their intensity via strong vibronic coupling of the Q_0-Soret transitions (Herzberg–Teller or *B*-term scattering[25]). The allowed symmetry of the vibronically active modes is $E_u \times E_u = A_{1g} + B_{1g} + B_{2g} + A_{2g}$ (in D_{4h} point group), and the bands attributed to the in-plane A_{2g} (ap) and the B_{1g}, B_{2g}(dp) modes of the porphyrin skeleton predominate in the 530.9- and 568.2-nm spectra, respectively (the A_{1g} (p) modes were shown to be ineffective in vibronic mixing[14]). The strong occurrence of the ap bands further supports the observation that the local core symmetry of NiTHBP's is not affected much by their alkyl substituents.

This differential enhancement pattern of the Raman bands in different scattering regimes of nickel tetrahydrobenzoporphyrins is very helpful in making band assignments, especially that it closely conforms to that of NiOEP for which detailed vibrational assignments have been achieved on the basis of multiple isotope substitution and rigorous normal mode calculations.[16a] In addition, the RR spectra of NiTHBP's may be thought of as the superposition of NiTBuP spectra on the corresponding NiEtio-III spectra. NiTHBP's are expected to show bands in common to NiEtio-III that involve methyl and ethyl substituents as well as vibrations due to the hydrocarbon exocycle rings of NiTBuP which does not have methyl or ethyl substituents. This is evident in Figures 3–6 which compare the RR spectra of NiEtio-III, NiTHBP-B, and NiTBuP in the regions between 900 and 1700 cm^{-1} (Figures 3–5) and between 150 and 900 cm^{-1} (Figures 6 and 7) obtained with 406.7-, 530.9-, and 568.2-nm excitation wavelengths which selectively enhance the polarized (p), anomalously polarized (ap), and depolarized (dp) Raman bands, respectively. All the observed RR frequencies and a qualitative assessment of depolarization ratios, ϱ, for four regioisomers of NiTHBP appear in Table 1 together with their assignments. The corresponding frequencies of NiTBuP are also included in Table 1, and the vibrational mode descriptions follow those of Li *et al.*[16a]

In-Plane Skeletal Modes and Structure in Solution. Careful examination of Table 1 indicates that the frequencies of the in-plane porphyrin skeletal modes (ν_i) are virtually indistinguishable among the A–D isomers of NiTHBP. Distinctions among these molecules stem from the Raman modes that involve the ethyl and methyl substituents and the vibrations of the exocycle ring bound to the pyrrole-C_β carbons and are discussed separately in the following sections. For most of the skeletal peaks, frequency differences are less than 2 cm^{-1} among the A–D isomers, which imply that the basic porphyrin core structure and the force constants governing the in-plane vibrational motions are not altered by a different disposition of the peripheral groups in these regioisomers. This is not too surprising because no significant electronic effect on the core

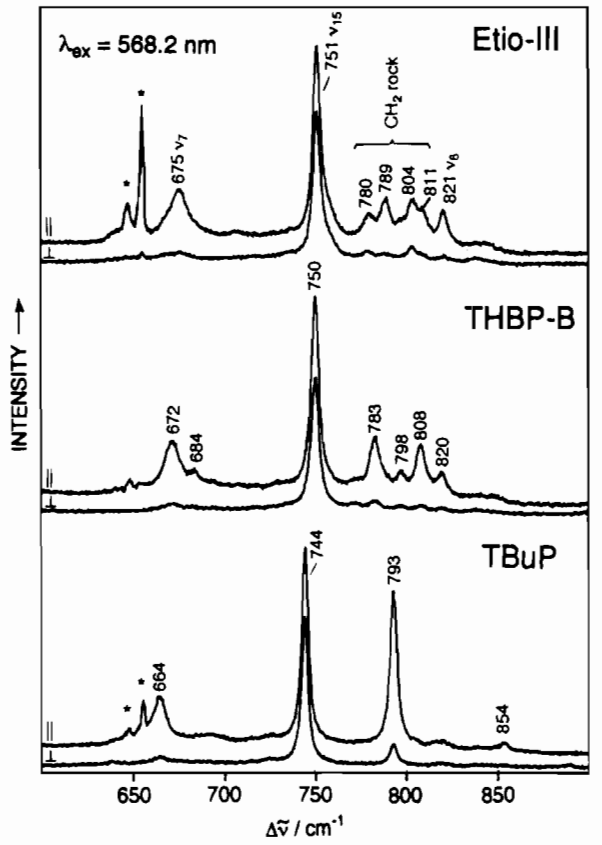

Figure 6. RR spectra in CS_2 of NiEtio-III (top), NiTHBP-B (middle), and NiTBuP (bottom), obtained with 568.2-nm (right) excitation wavelength in the 600−900-cm^{-1} region. CS_2 solvent bands indicated by asterisks. Conditions: backscattering from spinning NMR tube; 150-mW laser power; 2-cm^{-1} slit widths; average of three scans, 1-s integration time per data point at 0.5-cm^{-1} increments.

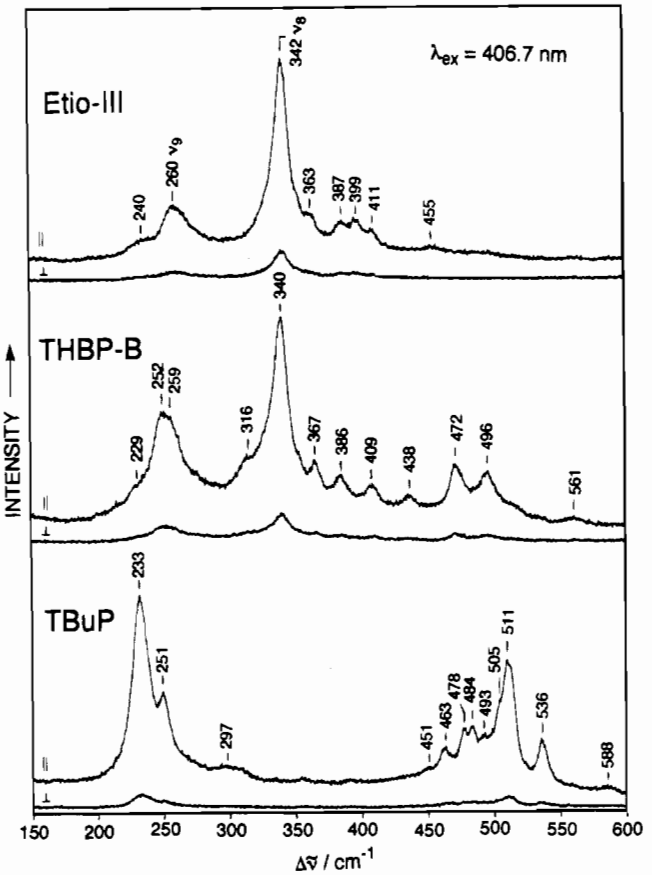

Figure 7. Same as in Figure 6, but with 406.7-nm excitation wavelength in the 150−600-cm^{-1} regions.

bonding is expected from a merely different arrangement of the equally electron-donating substituents, particularly given that all four regioisomers have the same overall symmetry (C_1). Indeed, as mentioned above, their absorption spectra are virtually identical (see Experimental Section). It is also clear that the kinematic couplings between the skeletal and the substituent modes, which could possibly be altered by different relative positions of the alkyl groups and thereby cause a change in the frequency, are not influenced very much either. Similar observations have been made for most of the skeletal vibrations of the NiEtio positional isomers I−IV[15,26] and of the pyrrole-N-substituted isomers of CuNΦPPDME (NΦPPDME = *N*-phenylprotoporphyrin IX dimethyl ester).[27] This is consistent with the detailed normal mode calculations of the porphyrin vibrational spectrum which have revealed a highly conserved nature of the main local normal coordinates contributing to each of the in-plane vibrations.[16a,28]

Compared in Figures 3−5 are the RR spectra excited at 406.7, 530.9, and 568.2 nm, respectively, for nickel complexes of Etio-III (top), THBP-B (middle), and TBuP (bottom) in CS_2 solution in the region between 900 and 1700 cm^{-1}. This region contains porphyrin structure-sensitive Raman lines, ν_2, ν_3, ν_4, ν_{10}, ν_{11}, ν_{19}, ν_{20}, ν_{28}, and ν_{29} (>1300 cm^{-1}), the frequencies of which were shown to be good indicators of macrocycle planarity.[11,16b,29] The intensity patterns are quite similar for the three porphyrin types, making band correspondences obvious. Nevertheless, to make sure that the bands are correlated properly, and to confirm their assignments, we substituted the methine-bridge hydrogen atoms with deuterium in NiTHBP-C and NiTBuP and recorded the CS_2 solution RR spectra of thus obtained isotopomers. The NiTHBP-C-d_4 and NiTBuP-d_4 spectra are not shown; however, the peak maxima (cm^{-1}) observed in both the natural abundance and d_4 samples of in-plane skeletal vibrations are tabulated in Table 2 and are arranged according to their symmetry blocks under idealized D_{4h} symmetry of the porphyrin basic core. The mode descriptions previously introduced by Li *et al.*[16a,28] are also given in Table 2. Also included for comparison purposes are the corresponding experimental frequencies (CS_2 solution) previously obtained for NiOEP and NiOEP-d_4.[16a] Among the NiOEP, NiTHBP, and NiTBuP porphyrins, the skeletal bands exhibit nearly analogous sensitivity to *meso*-deuteration; this result is anticipated since all β-pyrrole carbon atoms are substituted by alkyl groups. It is clear that the normal mode compositions of the in-plane skeletal vibrations do not differ much between these alkyl porphyrins, including NiEtio (Figures 3−5), despite noticeable differences in frequencies and *meso*-d_4 isotope shifts, ensuring the proposed vibrational assignments for tetrahydrobenzoporphyrins.

However, Table 3 shows that the differences displayed by skeletal bands above 1300 cm^{-1} are significant in that they are relatively consistent in trend; in the NiOEP complex, which is known to exist in the moderately nonplanar (ruffled) conforma-

(26) Rankin, J. G. Ph.D. Dissertation, University of Houston, 1993.
(27) Sparks, L. D.; Chamberlain, J. R.; Hsu, P.; Ondrias, M. R.; Swanson, B. A.; Ortiz de Montellano, P. R.; Shelnutt, J. A. *Inorg. Chem.* **1993**, *32*, 3153−3161.
(28) Li, X.-Y.; Czernuszewicz, R. S.; Kincaid, J. R.; Su, Y. O.; Spiro, T. G. *J. Phys. Chem.* **1990**, *94*, 31−47.
(29) (a) Spaulding, L. D.; Chang, C. C.; Yu, N.-T.; Felton, R. H. *J. Am. Chem. Soc.* **1975**, *97*, 2517−2525. (b) Alden, R. G.; Crawford, B. A.; Doolen, R.; Ondrias, M. R.; Shelnutt, J. A. *J. Am. Chem. Soc.* **1989**, *111*, 2070−2072. (c) Shelnutt, J. A.; Majumder, S. A.; Sparks, L. D.; Hobbs, J. D.; Medforth, C. J.; Senge, M. O.; Smith, K. M.; Miura, M.; Luo, L.; Quirke, J. M. E. *J. Raman Spectrosc.* **1992**, *23*, 523−529.

Table 1. Observed RR Frequencies (cm^{-1}) and Assignments for Ni(II) Complexes of Tetrahydrobenzoporphrins[a]

ϱ	THBP-A	THBP-B	THBP-C	THBP-D	TBuP	assgnt
dp[b]	1657	1657	1657	1657	1659	ν_{10} (B_{1g})
ap					1625	$\nu_{22} + \nu_g$
p	1606	1607	1607	1608	1611	ν_2 (A_{1g})
ap	1604	1604	1604	1604	1607	ν_{19} (A_{2g})
dp	1581	1582	1582	1580	1588	ν_{11} (B_{1g})
ap					1537	$\nu_{21} + \nu_9$
p	1521	1521	1522	1522	1524	ν_3 (A_{1g})
p	1499	1499	1499	1500	1488[c]	$2\nu_{15}$ (B_{1g})
dp	1485	1486	1485	1484	1488	ν_{28} (B_{2g})
ap	1463	1462	1463	1463		CH_2 scis-Et[d]
p	1458	1458	1458	1458		CH_2 scis-Et
p					1430	CH_2 scis-R
ap					1452/1445	CH_2 scis-R
dp	1415	1415	1415	1415	1420	ν_{29} (B_{2g})
ap	1401	1402	1401	1401	1410	ν_{20} (A_{2g})
p	1382	1381	1382	1381	1386	ν_4 (A_{1g})
p	1365	1366	1366	1366		CH_3 def-Et,Me
dp	1364	1366	1366	1365		CH_3 def-Et,Me
ap	1362	1361	1360	1364		CH_3 def-Et,Me
p	1345	1345	1346	1346	1344	CH_2 wag-R
p	1332	1331	1332	1333	1329	CH_2 wag-R
p	1312	1312	1310	1310		CH_2 wag-Et
ap	1305	1306	1305	1305	1306	ν_{21} (A_{2g})
dp					1297	CH_2 twist-R
ap	1288/1251	1288/1252	1288	1287/1251	1280/1244	CH_2 twist-R
dp	1270	1266/1271 sh	1266	1268		CH_2 twist-Et
ap	1264	1265	1263	1260		CH_2 twist-Et
p	1258	1258	1260	1260		CH_2 twist-Et
dp	1241	1239 sh	1239 sh	1239sh	1241/1253	CH_2 twist-R
dp	1226/1230 sh	1227	1227/1230 sh	1226	1229	ν_{13} (B_{1g})
p	1173	1173	1173	1173	1175	ν_5 (A_{1g})-R
dp	1173[e]	1173[e]	1173[e]	1173[e]	1165	ν_{14} (B_{1g})-R
dp	1159	1159	1159	1158	1153	ν_{30} (B_{1g})
p	1131/1144[f]	1132/1143[f]	1132/1143[f]	1131/1144[f]		ν_5 (A_{1g})
ap	1121 sh	1121sh	1121sh	1121 sh	1109	?
ap	1117	1117	1117	1117	1115	ν_{22} (A_{2g})
p	1092/1110	1092/1110	1092/1109	1092/1108	1099	ν(CC)-R
dp					1094	ν_{31} (B_{2g})
ap	1057	1060	1058	1060	1085/1046	ν_{23} (A_{2g})
p	1053/1073	1053/1073	1052/1073	1052/1072	1053/1072	ν(CC)-R
dp	1001	1008	1009	1008		ν_{31} (B_{2g})
dp	1001	1001	988	982		ν(CC)-Et
p	994	989	999	998		ν(CC)-Et
dp	978	978	976			ν_{45} (E_u)[g]
ap		950		951	951	ν_{45} (E_u)[g]
dp	947	948	948	949	948/964	ν_{32} (B_{2g})
dp	933/928 sh	929	928			ν_{46} (E_u)[g]
p			932	931	928	ν_{46} (E_u)[g]
p	908	908	910	909		?
ap	906/901	908	910	909/901	889	?
p	847	847/851	847/851	847/851	847/851	γ_4, oop[h]
ap	843	842	842	843	848	γ_{19}, oop
p	806[i]/821	809/813[i]/820	810/815/820 sh	802/808		CH_2,CH_3 rock
dp	809/772	798/772	797			CH_2,CH_3 rock
p	792	784	789	785	793	ν_6 (A_{1g})
p/dp					779/820	CH_2 rock-R
dp	757 sh	757 sh	757 sh			ν_{16} (B_{1g})
dp	749	750	749	750	745	ν_{15} (B_{1g})
p	707	708	708	708	713	$2\gamma_6$
p	685	684	684	685	687	γ_{21}, oop
p	672	672	672	672	664	ν_7 (A_{1g})
ap	592	594	593	593	638	ν_{24} (A_{2g})
p	558	561	554	553	562	ν_{49} (E_u)[g]
ap	560	560	559	558	606	ν_{25} (A_{2g})
p	533	535	535 sh	536 sh	536	$\delta(C_\beta CC)$-R
p	515	516	515	515	511	$\delta(C_\beta CC)$-R
p	501	496	493	498	504/493	$\delta(C_\beta CC)$-R
dp	486	484	484	488	491	ν_{33} (B_{2g})
p	471	472	479	476	484/478/463	$\delta(C_\beta CC)$-R
dp					467	$\delta(C_\beta CC)$-R
p	444	438	433	440		$\delta(C_\beta CC)$-Et
p	398/391	409/386	409/399	399	393	$\delta(C_\beta CC)$-R
p	364	367	367	371		$\delta(C_\beta CC)$-Et
dp	354	354	354	354	357	γ_6, oop
p	343	340	341	341		ν_g (A_{1g})

Table 1 (Continued)

ϱ	THBP-A	THBP-B	THBP-C	THBP-D	TBuP	assgnt
p	316	316	316	316	312	ν_{51} (E_u)[g]
dp	304	305	310	307	305	ν_{17} (B_{1g})
p	254	252	254/259	252		ν_9 (A_{1g})
p					251	ν_9 (A_{1g})-R
p	234	229	230	236	233	ν_8 (A_{1g})-R
dp	200 sh		200 sh	200 sh	185	ν_{34} (B_{2g})
dp	187	187	187	186	168[e]	ν_{18} (B_{2g})
dp		163 sh	161	164	168[e]	ν_{35} (B_{2g})

[a] Observed values from CS_2 and CH_2Cl_2 (600−700 cm^{-1}) solution RR spectra at room temperature (sh = shoulder). Assignments based on normal coordinate analysis for NiOEP (OEP = octaethylporphyrin).[16a] [b] p = polarized, dp = depolarized, and ap = anomalously polarized bands. [c] Overlaps with ν_{28} (1488 cm^{-1}); clearly more polarized in the 530.9-nm spectrum. [d] scis = scissors, wag = wagging, twist = twisting, rock = rocking, def = deformation, and C−C stretching modes of the methyl (Me) and ethyl (Et) groups and tetrahydrobenzo exocyclic rings (R). [e] Overlapping bands, as judged by mixed polarization. [f] Pairs of frequencies attributed to ν_5 involving C_β−C_1(Et) and C_β−C_1(Me) stretchings, respectively. [g] IR-active modes.[16a] [h] oop = out-of-plane modes.[16c] [i] Observed with 530.9-nm excitation.

Table 2. In-Plane Skeletal RR Frequencies (cm^{-1}) and Local Mode Assignments for Ni(II) Complexes of OEP, THBP-C, and TBuP and Their Meso-d_4 Isotopomers[a]

			OEP[c]		THBP-C		TBuP	
sym	ν_i	description[b]	na	d_4	na	d_4	na	d_4
A_{1g}	ν_2	$\nu(C_\beta-C_\beta)$	1602	1601	1607	1606	1611	1608
	ν_3	$\nu(C_\alpha-C_m)_{sym}$	1520	1512	1522	1515	1524	1517
	ν_4	ν(Pyr half-ring)$_{sym}$	1383	1382	1382	1382	1386	1386
	ν_5	$\nu(C_\beta-C_1)_{sym}$	1138	1138	1132	1122	1175	1175
	ν_6	ν(Pyr breath)	804	799	789	778	793	783
	ν_7	δ(Pyr def)$_{sym}$	674	668	672	666	664	
	ν_8	$\delta(C_\beta-C_1)_{sym}$	360/343[d]	353/343[d]	341	341	233	231
	ν_9	ν(Ni−N)	263/274[d]	262/274[d]	254	255	250	244
B_{1g}	ν_{10}	$\nu(C_\alpha-C_m)_{asym}$	1655	1645	1657	1647	1659	1649
	ν_{11}	$\nu(C_\beta-C_\beta)$	1577	1576	1582	1580	1588	1588
	ν_{12}	ν(Pyr half-ring)$_{sym}$		1331[e]		1321[e]		1315[e]
	ν_{13}	$\delta(C_m-H)$	1220	948	1227	944	1229	956
	ν_{14}	$\nu(C_\beta-C_1)_{sym}$	1131	1186	1173	1192	1165	1196
	ν_{15}	ν(Pyr breath)	751	683	749	681	744	672
	ν_{16}	δ(Pyr def)$_{sym}$	~740[f]	762	756	755/761		747[e]
	ν_{17}	$\delta(C_\beta-C_1)_{sym}$	305	305	310		305	
	ν_{18}	ν(Ni−N)	168	168	161	160	~168	~168
A_{2g}	ν_{19}	$\nu(C_\alpha-C_m)_{asym}$	1603	1581	1604	1584	1607	1589
	ν_{20}	ν(Pyr quarter-ring)	1393	1393	1401	1401	1410	1408
	ν_{21}	$\delta(C_m-H)$	1307	887	1305	884	1305	874
	ν_{22}	ν(Pyr half-ring)$_{asym}$	1121	1202	1117	1202	1115	1177
	ν_{23}	$\nu(C_\beta-C_1)_{asym}$	1058	1058	1058	1060	1085	
	ν_{24}	δ(Pyr def)$_{asym}$	597	582	593	586	638	639
	ν_{25}	δ(Pyr rot)	551	545	559		606	
B_{2g}	ν_{28}	$\nu(C_\alpha-C_m)_{sym}$	1483	1478	1485	1480	1488	1484
	ν_{29}	ν(Pyr quarter-ring)	1407	1405	1415	1412	1420	1418
	ν_{30}	ν(Pyr half-ring)$_{asym}$	1159	1159	1159	1158	1153	1153
	ν_{31}	$\nu(C_\beta-C_1)_{asym}$	1015	1003	1009	997	1094	
	ν_{32}	δ(Pyr def)$_{asym}$	938	934	949		948	944
	ν_{33}	δ(Pyr rot)	493	490	484		491	
	ν_{34}	$\delta(C_\beta-C_1)_{asym}$	197	197	187		185	184

[a] Mode frequencies from CS_2 solution RR spectra at room temperature. The unobserved C_m−H stretches, $\nu_1(A_{1g})$ and $\nu_{27}(A_{2g})$, and the $\delta(C_\beta-C_1)_{asym}$ bending, $\nu_{26}(B_{1g})$, are calculated at ~3000 and 245 cm^{-1} for NiOEP.[16a] [b] See ref 16a and 28 for local coordinates definitions. [c] Values from ref 16a. [d] Pairs of frequencies attributed to ethyl orientational isomerism.[16a] [e] Observed in the *meso*-d_4 isotopomers only. [f] Observed in 12 K RR spectra of tetragonal crystals.[16c]

Table 3. RR Frequencies (cm^{-1}) of the Structure-Sensitive Marker Bands for Ni(II) Complexes of OEP, Etio-I−IV, THBP-A, B, and TBuP in CS_2 Solution

porphyrin	ν_2	ν_3	ν_4	ν_{10}	ν_{11}	ν_{19}	ν_{20}	ν_{28}	ν_{29}
OEP[a]	1602	1520	1383	1655	1577	1603	1393	1483	1407
OEP-flat[b]	1608	1523	1383	1663	1581	1609	1395	1485	1408
OEP-ruffled[b]	1595	1512	1383	1642	1572	1589	1391	1476	1406
Etio-I[c]	1607	1522	1380	1656	1580	1604	1401	1482	1411
Etio-II[d]	1607	1522	1381	1655	1579	1603	1398	1484	1409
Etio-III[c]	1605	1520	1380	1656	1579	1603	1399	1485	1411
Etio-IV[d]	1604	1521	1381	1654	1578	1602	1399	1483	1409
THBP-A	1606	1521	1382	1657	1581	1604	1401	1485	1415
THBP-B	1607	1521	1381	1657	1582	1604	1402	1486	1415
THBP-C	1607	1522	1382	1657	1582	1604	1401	1485	1415
THBP-D	1608	1522	1381	1657	1580	1604	1401	1484	1415
TBuP	1611	1524	1386	1659	1588	1607	1410	1488	1420

[a] From ref 16a. [b] Triclinic (flat NiOEP) and tetragonal (ruffled NiOEP) crystal forms in KCl pellets; from ref 16c. [c] From ref 15. [d] From ref 26.

tion(s) in solution,[16b,29b] the 1655- (ν_{10}), 1603- (ν_{19}), 1602- (ν_2), 1577- (ν_{11}), 1520- (ν_3), 1483- (ν_{28}), 1407- (ν_{29}), 1393- (ν_{20}), and 1383-cm^{-1} (ν_4) lines are all markedly shifted up, to 1659, 1611, 1607, 1588, 1524, 1488, 1421, 1410, and 1386 cm^{-1}, respectively, in the NiTBuP complex, with the corresponding lines of NiEtio and NiTHBP isomers falling between those of NiOEP and NiTBuP. Inasmuch as these bands arise from vibrations involving primarily stretching of the pyrrole and methine bridge double bonds,[16a] this trend of increasing frequencies, NiOEP < NiEtio's < NiTHBP's < NiTBuP, is indicative of increasing π-conjugation and, in turn, planarity of the porphyrin macrocycle in the series. Reference to Figures 3−5 also yields the observation that the half-bandwidth of the structure-sensitive bands decreases substantially with increasing vibrational frequency, further supporting subtle structural differences between the porphyrin macrocycles in these metalloporphyrins. The structure-sensitive modes of the NiTHBP regioisomers are only slightly upshifted (0−3 cm^{-1}) relative to those modes of the NiEtio isomers (Table 3). This implies a similar, if not slightly more planar, conformation of the THBP macrocycles in solution relative to NiEtio's and a small influence of the fused hydrocarbon ring on these skeletal vibrations regardless of where this ring is located. Structure-sensitive modes of NiTBuP in solution are all much closer in frequency to those found in orthorhombic NiEtio-III[26] and triclinic NiOEP[30a,b] crystals composed of planar porphyrin molecules than to those of the tetragonal NiOEP crystals[30c] containing ruffled NiOEP (Table 3).[16b,28a,25] This contrasts $NiTC_6TPP$, a derivative of NiTBuP bearing phenyl groups at the *meso*-carbon atoms instead of hydrogens, which was shown to be highly nonplanar in crystals as well as solution.[11] The RR data also indicate that the NiTHBP isomers appear to be slightly less planar than NiTBuP as evidenced by the lower frequencies (2−6 cm^{-1}) of their structure-sensitive modes above 1300 cm^{-1} (Table 3). The slight blue shift of the electronic absorption spectrum of NiTBuP relative to NiTHBP isomers also supports this observation.[29b]

Of the mid- and low-frequency in-plane skeletal modes of NiTHBP isomers, only those modes whose calculated potential energy distribution (PED) involve substituent coordinates[16a] have

(30) (a) Cullen, D. L.; Meyer, E. F. *J. Am. Chem. Soc.* **1974**, *96*, 2095−2102. (b) Brennan, T. D.; Scheidt, W. R.; Shelnutt, J. A. *J. Am. Chem. Soc.* **1988**, *110*, 3919−3924. (c) Meyer, E. F. *Acta Crystallogr., Sect. B* **1972**, *B28*, 2162−2167.

shown significant deviations from NiEtio-III or NiOEP. These skeletal modes are discussed below along with the substituents involved.

Exocyclic Ring Modes. A comparison of the RR spectra of NiEtio-III, NiTHBP-B, and NiTBuP reveals that a number of bands in both the low- and high-frequency regions of NiTHBP's can be attributed to the vibrational modes which are predominantly β,β-butano ring in character (Table 1). These modes gain intensity upon excitation in resonance with both the Soret and Q-bands, suggesting significant electronic involvement of the tetrahydrobenzo (THB) unit(s) in the porphyrin $\pi-\pi^*$ excited states. Saturated hydrocarbon substituents are not normally thought to couple electronically to aromatic chromophores, and therefore, it was commonly assumed that the modes of these groups do not contribute to the RR spectra of porphyrins. However, recent RR studies on methylene-perdeuterated NiOEP[16a] have revealed that the internal ethyl vibrations of OEP, particularly those involving stretching of the (outer) ethyl C_1-C_2 bonds ($\sim$1020 cm^{-1}) and methylene deformations ($\sim$800 and >1200 cm^{-1}), are strongly enhanced with both the Soret- and Q-band excitations. Furthermore, normal mode calculations on NiOEP, which involved explicit inclusion of the ethyl internal coordinates, showed quite small porphyrin skeletal coordinate contributions to the PED of the ethyl assignable vibrations.[16a] Thus, the RR activity of these vibrations has been attributed to hyperconjugation of the alkyl groups with the porphyrin ring,[16a] presumably by mixing of ethyl σ character into the porphyrin π^* orbitals.[31]

The methylene deformation (CH_2 scissors) is expected at $\sim$1450 cm^{-1},[32] and weak bands are seen near this frequency for NiTBuP which are polarized (1430, 1452 cm^{-1}), anomalously polarized (1445 cm^{-1}), and depolarized (1445 cm^{-1}) with 406.7-, 530.9- and 568.2-nm excitations, respectively. These bands are too weak to be detected in the NiTHBP spectra; instead two weak features in this region, at 1458 (p) and 1463 (ap) cm^{-1}, are assigned to the CH_2 scissor modes of the ethyl groups (Table 1) in agreement with the identical bands seen for NiEtio-III.[15]

Methylene wagging and twisting modes cover a range of frequencies in different compounds but are generally not far from 1300 cm^{-1} in alkyl groups.[33] A polarized band is found for NiTHBP and NiEtio-III at $\sim$1310 cm^{-1}, but not for NiTBuP, and is therefore assigned to CH_2 wagging of ethyl substituents (Table 1). In addition, two polarized bands at 1332 and 1345 cm^{-1} are clearly located in the Soret-excited spectrum of NiTHBP (Figure 3, middle) which are absent in the NiEtio-III spectrum (top). These two bands, which occur at 1329 and 1344 cm^{-1} in NiTBuP with more than half the intensity of the ν_4 band (1386 cm^{-1}), are consistent with the two polarized bands seen previously in cyclohexene.[33] Although they did not make assignments in this region, Shelnutt *et al.* also observed similar bands at 1331 and 1360 cm^{-1} in their RR study of $NiTC_6TPP$.[11] Because the calculated PED values for the cyclohexene modes in this region indicate a wagging motion,[33] we assign the $\sim$1330- and 1345-cm^{-1} bands of NiTHBP and NiTBuP, as well as the 1330- and 1360-cm^{-1} bands of $NiTC_6TPP$, to CH_2 wagging of the exocyclic ring methylene groups.

Polarized, depolarized, and anomalously polarized bands, assignable to the CH_2 twisting modes of the Etio and THBP ethyl substituent groups, are found at 1250−1275 cm^{-1} by comparison of the NiEtio-III and NiTHBP spectra (Figures 3−5). This assignment is consistent with the 1250−1280-cm^{-1} band assignments in NiOEP.[16a] Several NiTHBP bands in the same region, which do not appear in the NiEtio-III spectra, but which intensify in the NiTBuP spectra, have been identified with the CH_2 twisting modes of the exocyclic ring methylenes (Table 1).

The new polarized band at 1173 cm^{-1} in the Soret-excited spectrum of NiTHBP-B (Figure 3, middle), which is absent in the NiEtio-III spectrum (top), is assigned to the $C_\beta-C_1$ symmetric stretching vibration, $\nu(C_\beta C_1)$, where C_1 is the benzylic carbon of the butano ring corresponding to the ν_5 skeletal mode at 1132 cm^{-1} where C_1 is the methylene carbon of the ethyl substituents (1136 cm^{-1} in NiEtio-III[15]). The 1132-cm^{-1} band totally disappears in NiTBuP whereas the 1173-cm^{-1} band dramatically intensifies and shifts only slightly upward, to 1175 cm^{-1} (Figure 3, bottom). No such band is found in NiEtio's[15,26] or NiOEP,[16a] confirming its assignment as the ν_5-like mode involving the β,β-butano substituent, $\nu(C_\beta C_1)$-R. The corresponding B_{1g} mode, ν_{14}, appears to be accidently degenerate with ν_5 at 1173 cm^{-1}, as the 1173-cm^{-1} band in the 568.2-nm-excited spectrum (Figure 5, middle) displays a mixed polarization ($\varrho \sim 0.5$). However, in NiTBuP the two modes are clearly resolved into two bands, a polarized one at 1175 cm^{-1} (ν_5) and a depolarized one at 1165 cm^{-1} (ν_{14}) (Figure 5, bottom). An alternative band for ν_{14} could be a shoulder at $\sim$1143 cm^{-1} (a relatively weak dp band was observed at 1139 cm^{-1} in cyclohexene[33]), but no corresponding band is found in NiTBuP.

The most distinguishing feature associated with the tetrahydrobenzo ring in NiTHBP's is the polarized band found at 1092 cm^{-1} which is particularly strong with a 568.2-nm excitation wavelength (Figure 5). When the pyrrole ethyl and methyl substituents of NiTHBP are all replaced with the β,β-butano groups in NiTBuP, this band moves upward to 1099 cm^{-1} and becomes the strongest feature in the 568.2-nm spectrum, indicating a common vibrational mode for the 1092- (THBP) and 1099-cm^{-1} (TBuP) RR bands. Previously, such a situation has been found for the $\sim$1000-cm^{-1} band of NiEtio isomers arising from the ethyl C_1-C_2 stretching,[15,26] where it also shifts upward, to 1024 cm^{-1}, and drastically gains intensity in NiOEP[16a] upon exchange of the four Etio methyl substituents with the ethyl groups in OEP. The $\nu(C_1C_2)$ assignment of the 1024-cm^{-1} band in NiOEP has been secured by methylene-d_{16} substitution and normal mode calculations.[16a] Thus, the 1092- (NiTHBP) and 1099-cm^{-1} (NiTBuP) RR bands are assigned to the C−C stretch of the tetrahydrobenzo ring, ν(CC)-R, corresponding to $\nu(C_1C_2)$ of terminal ethyls found near 1000 and 1024 cm^{-1} for NiEtio's and NiOEP, respectively. Other weaker features of NiTHBP's at ca. 1053 and 1073 cm^{-1} are also assigned to C−C stretching modes of the exocyclic ring; these Raman lines intensify in NiTBuP (see Figure 5), and thus they do not involve methyl or ethyl terminal substituents. In addition, similar features are observed and calculated in this region for cyclohexene.[33] Hence, the 1092-cm^{-1} exocycle band of the model NiTHBP's, and those at 1053 and 1073 cm^{-1}, provide especially unique structural marker bands for nickel, as well as vanadyl, tetrahydrobenzoporphyrins in oil shales and petroleum.

Figure 6 compares the RR spectra of NiEtio-III, NiTHBP (isomer B), and NiTBuP measured at 568.2-nm excitation in the frequency range from 600 to 900 cm^{-1}. For alkyl porphyrins, *meso*-d_4-sensitive pyrrole breathing ν_6 ($\sim$800 cm^{-1}, p) and ν_{15} ($\sim$750 cm^{-1}, dp) and symmetric pyrrole deformation ν_7 ($\sim$670 cm^{-1}, p) and ν_{16} ($\sim$750 cm^{-1}, dp) vibrational modes occur strongly in this region, along with the *meso*-d_4-insensitive

(31) Libit, L.; Hoffman, R. J. *J. Am. Chem. Soc.* **1974**, *96*, 1370−1383.
(32) Colthup, N. B.; Daly, L. H.; Wiberly, S. E. *Introduction to Infrared and Raman Spectroscopy*, 3rd ed.; Academic Press: Boston, MA, 1990.
(33) Neto, N.; Di Lauro, C.; Castellucci, E.; Califano, S. *Spectrochemica Acta* **1967**, *23A*, 1763−1774.

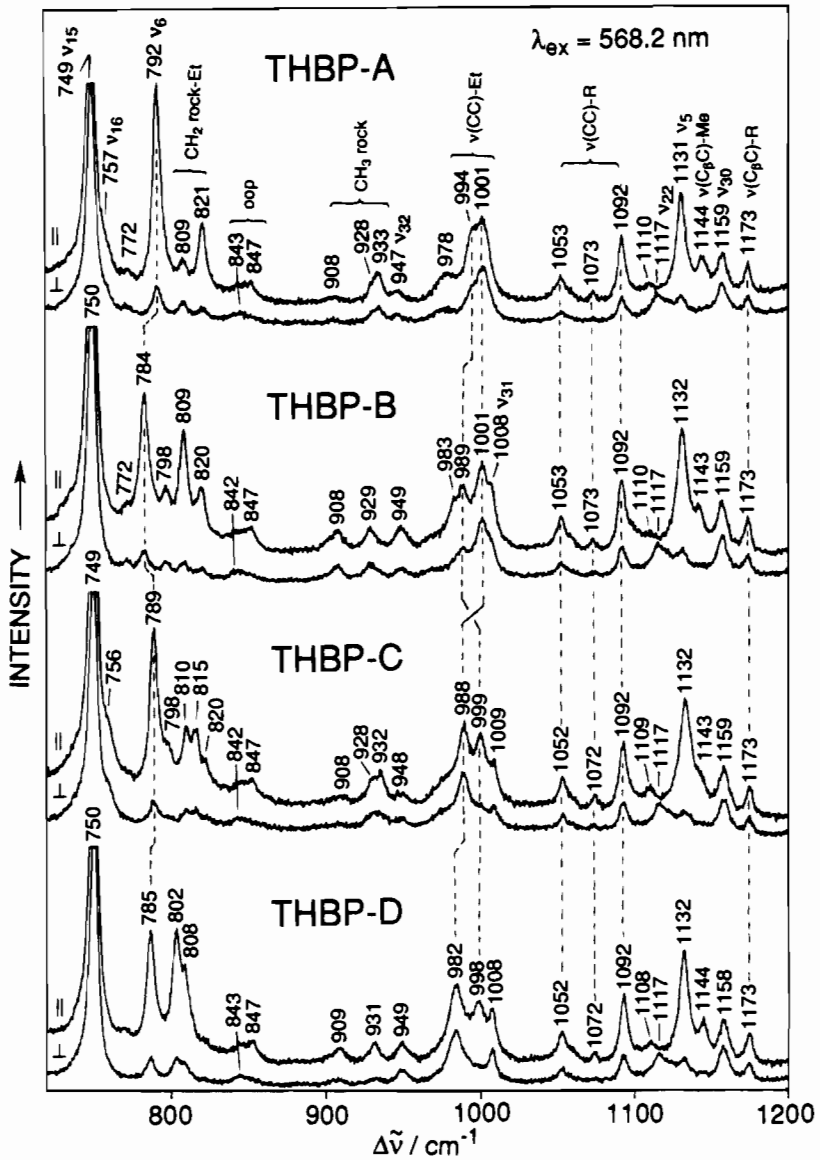

Figure 8. Details of the 568.2-nm-excited RR spectra (CH_2Cl_2 solution) in the 720−1200-cm^{-1} region for nickel(II) complexes of all four tetrahydrobenzoporphyrin regioisomers. Conditions are as in Figure 6.

methylene rocking motions (~750-820 cm^{-1}).[15,16a] The ν_7 and ν_{15} modes of NiTHBP are readily identified with the bands at 672 (p) and 750 (dp) cm^{-1} (749 cm^{-1} in isomers A and C), respectively, on the basis of their polarization properties and the 6- (ν_7) and 68-cm^{-1} (ν_{15}) *meso*-d_4 isotope shifts to lower frequencies in NiTHBP-C-d_4 (Table 2). The skeletal mode, ν_6, found at 804 cm^{-1} in NiOEP and 799 cm^{-1} in NiOEP-d_4, has a calculated PED of ~30% $\nu(C_\beta\text{-}C_1)$ character in NiOEP;[16a] thus, a counterpart involving exocyclic ring(s) coordinates is to be expected. As with NiEtio-III, there are a number of possible candidate bands for ν_6, both alkyl as well as ring, in this region for NiTHBP-B (Figure 6, middle). Further the alkyl CH_2 rocking modes are expected here (Table 1). In the NiTBuP spectrum (Figure 6, bottom), only a single strong polarized band is observed at 793 cm^{-1} and is thus assigned to ν_6. For NiTHBP-B the most intense polarized band at 783 cm^{-1} is also assigned to ν_6. The assignment of the 793-cm^{-1} band in NiTBuP is supported by a 10-cm^{-1} shift to lower frequency upon *meso*-d_4 substitution, in agreement with the 5-cm^{-1} shift observed for the ν_6 mode at 804 cm^{-1} in NiOEP.[16a]

The low-frequency region (150-600 cm^{-1}) of the Soret-excited spectrum of NiTHBP's, shown in Figure 7 for isomer B (middle), contains a number of broad polarized bands between 450 and 550 cm^{-1} which are not seen in NiEtio-III (top). Again, these bands intensify and become more complex in NiTBuP (Figure 7, bottom) and are therefore attributed to exocyclic ring deformation modes; both in-plane and out-of-plane deformation modes have been observed and calculated in this region for cyclohexene.[33] Additional, depolarized bands assigned to exocyclic ring deformation modes are observed with Q-band excitations (Table 1). All these bands showed little sensitivity to *meso* deuteration as expected for modes being predominantly exocyclic in character. The remaining bands in the low-frequency region have been assigned to in- and out-of-plane porphyrin skeletal modes[16c] as indicated in Figure 7 and Table 1. Thus for example, the prominent polarized bands assigned to in-plane ν_8 and ν_9 skeletal modes in NiEtio-III[15] at 342 and 260 cm^{-1}, respectively, are also seen in NiTHBP-B at 340 and 259/252 cm^{-1}, but for NiTBuP, the ν_8 mode appears to move down into the ν_9 mode region where now two strong polarized bands are seen at 233 and 251 cm^{-1} (Figure 7). The ν_8 and ν_9 modes are calculated to be strongly coupled Ni−pyrrole breathing and C_β−ethyl bending motions in NiOEP,[16a] and these bands are expected to be sensitive to the C_β−C−C angles and orientations. Selective isotopic labeling of the butano ring(s)

along with normal mode calculations will be necessary to confirm these assignments.

NiTHBP Regioisomerism. In Figure 8, the 568.2-nm-excited RR spectra are compared for four regioisomers of NiTHBP in the region between 725 and 1200 cm^{-1}. Similarly to NiEtio isomers,[15,26] these spectral regions and excitation wavelengths are best for distinguishing the four isomers from each other and from other petroporphyrins. Although characteristic for tetrahydrobenzoporphyrin structure, the frequencies of the Raman bands arising from vibrations involving an exocyclic ring, $\nu(C_\beta C_1)$-R at 1173 cm^{-1} and ν(CC)-R at 1092, 1073, and 1053 cm^{-1}, are not sensitive to where the ring is located on the porphyrin macrocycle. In contrast, the bands in the 800−1000-cm^{-1} range, which are mainly due to the terminal alkyl substituent modes and a pyrrole breathing mode ν_6 (Table 1), change markedly with the location of the THB ring on the porphyrin macrocycle, each NiTHBP isomer showing a uniquely distinctive vibrational signature (see Figure 8). A comparison of the four spectra reveals, for example, an interesting pattern of bands clustered near 1000 cm^{-1} which originates from the symmetric (p) and antisymmetric (dp) combinations of ethyl C_1-C_2 stretching, ν(CC)-Et, and a porphyrin skeletal mode ν_{31}.[15,16a] The ν_{31} mode, which involves C_β−alkyl stretching, is identified with a dp band at 1009 cm^{-1} in NiTHBP-C on the basis of its 12-cm^{-1} *meso*-d_4 shift (Table 2). Isomers B and D display similar dp bands at 1008 cm^{-1}, but the ν_{31} mode is not discernible in the spectrum of isomer A, most likely falling under the dp ν(CC)-Et band at 1001 cm^{-1} (Figure 8, top). More significantly, however, there is a characteristic crossing of the polarized and depolarized ν(CC)-Et bands which appears to correlate with a relative disposition of the ethyl substituents among the four NiTHBP porphyrins. It can be noticed that isomers A and B bear a pair of ethyl groups at the adjacent pyrrole-C_β positions (pyrroles C and D, Figure 1) and the depolarized ν(CC)-Et bands occur at higher frequency, 1001 cm^{-1} in both, with the polarized counterpart appearing at lower frequency, 984 cm^{-1} in A and 989 cm^{-1} in B. This vibrational pattern is reversed in the RR spectra of isomers C and D which do not have ethyl groups on adjacent C_β positions; the ν(CC)-Et dp component is pushed down to 988 and 982 cm^{-1} in NiTHBP-C and -D, respectively, and the p components are shifted up to ~999 cm^{-1} (Figure 8). The former pattern is reminiscent of NiEtio-II, which has two (C_2 axis-related) pairs of adjacent ethyls, and the 999- and 900-cm^{-1} ν(CC)-Et bands are depolarized and polarized, respectively.[15] Thus it appears that if two ethyl substituents are adjacent and can interact, the dp band is higher in frequency than the p band. This same occurrence will be seen again in the forthcoming paper, where all of the NiCAP's have adjacent ethyls in the "top half" like NiEtio-II and have the dp band at ~1000 cm^{-1}.[17]

The 900−950-cm^{-1} region shows an interesting pattern as well, with similar intensities of three dp bands in NiTHBP-B and -D, ~980, ~930, and 949 cm^{-1}, but only one larger, mainly p, band (~932 cm^{-1}) with much weaker dp side bands in isomers A and C (Figure 8). Band is this region have been assigned to methyl rocking modes in NiOEP and NiEtio's along with the skeletal mode ν_{32} which has been calculated to involve C_β−ethyl bending motions in NiOEP.[15,16a] We notice that the substituent methyl and ethyl groups of the B and D pyrrole rings may be related by the local symmetry of a C_2 axis running through the β,β-butano ring and opposite pyrrole in the A and C forms but are not in the B and D forms. This local symmetry may account for the pattern in this region.

The ~800-cm^{-1} region in the RR spectra of NiTHBP isomers contains a series of polarized bands as complicated as those in NiEtio-III (Figure 6) but clearly shows differences unique for each positional isomer (Figure 8). As discussed above, with the higher symmetry of NiTBuP (like NiEtio-I and NiOEP), bands in this region collapse into one single polarized band (793 cm^{-1}) which is assigned to the pyrrole breathing mode ν_6 on the basis of its 10 cm^{-1} *meso*-d_4 downshift (Table 2). The strongest polarized band found between 783 and 792 cm^{-1} in the mono-β,β-butano isomers is likewise assigned to ν_6, on the basis of the similar *meso*-d_4 sensitivity observed for the 789-cm^{-1} peak of NiTHBP-C (Table 2). The other bands in this region are probably methylene rocking vibrations[16a,32] whose number and frequencies are clearly influenced by the positional relationships of the alkyl groups to the tetrahydrobenzo ring. More detailed description of the 700−1200-cm^{-1} spectral region is given elsewhere.[15b]

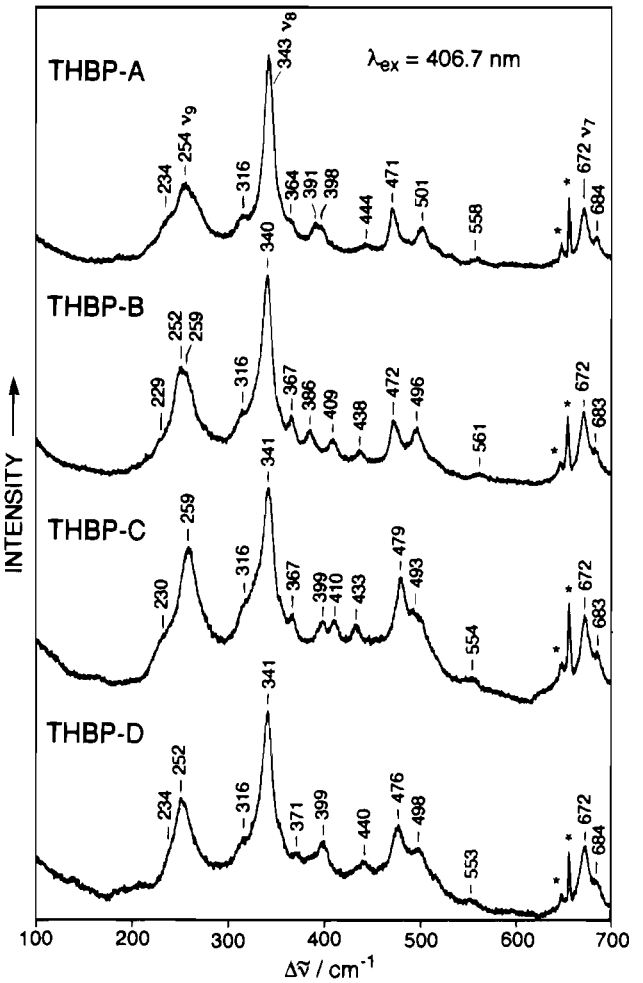

Figure 9. 406.7-nm-excited RR spectra (CS_2 solution) in the low-frequency region (100−700 cm^{-1}, parallel scattering components only) for nickel(II) complexes of all four tetrahydrobenzoporphyrin regioisomers. Solvent bands are indicated by asterisks. Conditions are as in Figure 6.

Finally, a series of weak polarized bands are seen between 360 and 450 cm^{-1} which can also be used to distinguish the four NiTHBP regioisomers (Figure 9), although not as well as the Q-band excited RR spectra in the 600−1200 cm^{-1} region (Figures 6 and 8) discussed above. Bands in the same region are assigned to primarily C_β−alkyl deformation and porphyrin out-of-plane modes for NiEtio isomers.[26]

Conclusions

The structure-sensitive in-plane skeletal RR bands in the high-frequency region of NiTHBP spectra are almost identical among

the four regioisomers and similar, though slightly upshifted, to those of the NiEtio's. These same bands in NiTBuP are upshifted in frequency even more implying a more planar porphyrin macrocycle.

A number of bands have been assigned to vibrational modes of the exocyclic ring in NiTHBP's. Most distinctive is a moderately strong, polarized band at 1092 cm^{-1} (1099 cm^{-1} in NiTBuP) which has been assigned to C−C stretching of the exocycle. This band is unique among the petroporphyrins studied so far. A second marker band for tetrahydrobenzoporphyrins is found at ~1173 cm^{-1} (1175 cm^{-1} in NiTBuP) which is assigned to $\nu(C_\beta C_1)$-R.

The four regioisomers can be readily differentiated by the frequencies and polarizations of bands in the 900−1000- and 780−820-cm^{-1} regions where ethyl and methyl substituent modes occur. Interaction of these substituents with the β,β-butano ring and differences in local symmetries are postulated as being responsible for the particular patterns observed.

Acknowledgment. This work was supported by the University of Houston President's Research and Scholarship Fund (PRSF) and in part by Grant E-1184 from the Robert A. Welch Foundation (to R.S.C.). T.D.L acknowledges support from the National Science Foundation under Grant No. CHE-9201149. Receipt of a Texaco Graduate Research Fellowship (J.G.R.) is gratefully acknowledged.

IC950023S